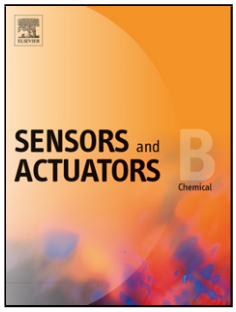


Title: Highly sensitive volatile organic compounds vapour measurements using a long period grating optical fibre sensor coated with metal organic framework ZIF-8

Authors: Jiri Hromadka, Begum Tokay, Ricardo Correia, Stephen P. Morgan, Sergiy Korposh

PII: S0925-4005(18)30015-7
DOI: https://doi.org/10.1016/j.snb.2018.01.015
Reference: SNB 23912

To appear in: *Sensors and Actuators B*

Received date: 10-7-2017
Revised date: 29-12-2017
Accepted date: 2-1-2018

Please cite this article as: Jiri Hromadka, Begum Tokay, Ricardo Correia, Stephen P.Morgan, Sergiy Korposh, Highly sensitive volatile organic compounds vapour measurements using a long period grating optical fibre sensor coated with metal organic framework ZIF-8, Sensors and Actuators B: Chemical https://doi.org/10.1016/j.snb.2018.01.015

# Highly sensitive volatile organic compounds vapour measurements using a long period grating optical fibre sensor coated with metal organic framework ZIF-8

Jiri Hromadka[1,2], Begum Tokay[3], Ricardo Correia[1], Stephen P Morgan[1] and Sergiy Korposh[1]

[1]*Optics and Photonics Group, Faculty of Engineering, University of Nottingham, University Park, Nottingham NG7 2RD, United Kingdom*

[2]*Institute for Environmental Studies, Faculty of Sciences, Charles University in Prague, Benátská 2, CZ 12843 Praha 2, Czech Republic*

[3]*Chemical and Environmental Engineering Department*, *Faculty of Engineering, University of Nottingham, University Park, Nottingham NG7 2RD, United Kingdom*

## Highlights

- An optical fibre long period grating VOCs sensor coated with ZIF8 reported
- In-situ crystallization of ZIF8 thin film synthesis is conducted
- A concentration specific response to acetone, ethanol and methanol vapour was obtained
- The optimized sensor shows a LOD of 6.67 and 5.56 ppm for acetone and ethanol respectively

## Abstract

An optical fibre long period grating (LPG) based volatile organic compound (VOC) sensor coated with ZIF-8, a material from the zeolite imidazolate framework (ZIF) family, functional coating is presented. ZIF-8 film was deposited onto the surface of the LPG using an in-situ crystallization technique by mixing freshly prepared 12.5 mM zinc nitrate hexahydrate and 25 mM 2-metyl-imidazole solutions in methanol. A concentration specific response to acetone, ethanol and methanol vapour was obtained over the high concentration range up to tens thousands ppm. The LPG based sensor works at phase-matching turning point (PMTP) and such operates at the highest sensitivity. A novel approach for the data analysis based on the measurement of the bandwidth of the U-shaped attenuation band of the LPG is introduced. The optimized sensor shows a sensitivity of 0.015±0.001 and 0.018±0.0015 nm/ppm and limit of

detection (LOD) of 6.67 and 5.56 ppm for acetone and ethanol respectively.

**Key words:** Long period grating (LPG), metal organic framework (MOF), ZIF-8, volatile organic compounds (VOCs) sensor, ethanol, methanol, acetone

## 1. Introduction

The fabrication of low-cost, portable, accurate and real-time sensors for organic vapour detection is of considerable interest in biomedical fields and in food quality monitoring (1). Ethanol and acetone represent the most common examples of volatile organic compounds (VOCs). The measurement of ethanol in breath is of high interest in traffic safety (2), where the accepted alcohol limits in blood vary across Europe from 0.2 to 0.8 ‰, which corresponds to a concentration of 30 to 130 ppm in breath (2). The detection of acetone in breath is important in medical diagnostics, where the increase of acetone concentration (single ppm units) can be related to diabetes (3) and high concentration (tens-hundreds ppm) is observed as symptom of ketoacidosis (4). VOCs are usually measured using gas chromatography – mass spectroscopy (GC-MS), however, the detection is expensive and needs experienced personnel (5). Currently, most ethanol sensors are based on metal oxide semiconductors such as $SnO_2$ (6), $WO_3$ (7), $In_2O_3$ (8), $Fe_2O_3$ (9) and ZnO (10). Semiconducting material based sensors exhibit high sensitivity whilst they usually operate at high temperatures (200–400 °C) to achieve chemical reactivity between the sensing material and the target gases. Also the fabrication of the sensitive layer should be conducted at high temperature and thus is associated with high energy consumption (11,12).

Fibre-optic sensing platforms are small, lightweight, immune to electromagnetic interference and as such can be used in extreme conditions, enabling remote real time monitoring with no electrical power needed at the sensing point (13). There have been a number of fibre-optic based ethanol gas sensors proposed recently using the deposition of the sensitive layer on the fibre tip to form Fabry-Perot interferometers (14–18) or evanescent wave sensors, where part of the cladding is mechanically or chemically removed and then the functional coating is deposited over the stripped region (11,19–22). A coating sensitive to ethanol vapours has been also applied on the surface of a photonic crystal fibre (23), long period grating (LPG) (24) or quartz crystal microbalance (QCM). The properties of published ethanol gas fibre optic based sensors (and one example of a QCM) are summarized in Table 1**.** Reported sensors suffer

mostly from a high response time in a range of 10s minutes (19,24) and are usually tested over a limited concentration range. For example, they are tested at saturated vapour conditions (18,24), high (in a range of thousands of ppm) (22,23,26) or low level concentrations usually below 500 ppm (11,14,19–21). The comparison in sensitivity shown in Table 1 is limited as only two papers show the limit of detection of 2.74 (16) and 380 ppm (17).

Among the different types of fibre-optic sensors, those based on gratings, specifically LPGs, have been employed extensively for refractive index measurements (27) and for monitoring associated chemical processes (27), since they offer wavelength-encoded information which overcomes the referencing issues associated with intensity based approaches. A LPG consists of a periodic perturbation of the refractive index of the fibre core, which couples the core mode to the co-propagating cladding modes of the fibre. This coupling is manifested in the transmission spectrum of the optical fibre as a series of resonance bands. Each resonance band corresponds to coupling to a different cladding mode and thus shows different sensitivity to environmental changes (28). The coupling wavelength can be obtained from the following phase matching equation

$$\lambda_x = (n_{core} - n_{clad(x)})\Lambda \qquad \text{[EQ 1]}$$

where $\lambda_x$ represents the wavelength at which light is coupled to the $LP_{0x}$ cladding mode, $n_{core}$ is the effective refractive index of the mode propagating in the core of the fibre, $n_{clad(x)}$ is the effective index of the $LP_{0x}$ cladding mode and $\Lambda$ is the period of the LPG (28). The central wavelength of the resonance band is sensitive to changes in the surrounding environment such as temperature or external index of refraction (28). It has been shown that the phase matching condition for the higher order cladding modes contains a turning point and that the LPG exhibits the highest sensitivity when phase matching turning point (PMTP) is reached. At PMTP the U-shaped attenuation band growth larger (i.e. transmission decreases) and then splits into two bands that move into opposite directions. Measurements of the wavelengths separation or width of the band, as will be shown in this work, allows to achieve higher sensitivity. This can be achieved by choosing an appropriate LPG period and coating thickness (29)(30). The cladding modes associated with the attenuation bands have been calculated through numerical modelling using the phase matching equation and weakly guided approximation to determine the effective refractive indices of the core and cladding modes and the known values of the central wavelengths and the grating period (31).

The key element of a LPG based chemical sensor is the sensitive layer that captures the analyte. It has been shown that metal organic frameworks (MOFs), because of their unique properties, such as high surface area, adjustable shape and size of the pores and inner cavities, offer an ideal platform for the development of this sensitive layer (32–34). The sensing mechanism of the LPG towards VOCs is based on the change of the refractive index of the sensitive layer due to the analyte of interest. It is therefore important to select MOFs that provide a specific and sensitive change in refractive index. Among the variety of MOFs, a zeolitic imidazole framework (ZIF) - ZIF-8 possesses properties that show promise for sensor development, such as its chemical robustness and thermal stability due to the sodalite (SOD) type of structure. The structure of ZIF-8 comprises zinc ions coordinated by four imidazolate rings with large cavities (11.6 Å) and small pore apertures (3.4 Å) (35) which provides sensitivity to small molecule VOCs. ZIF-8 has been considered to behave as an adsorbent with molecular sieving properties. An investigation of a ZIF-8 film demonstrated the adsorption of isopropanol in a selective manner versus water (36). A ZIF-8 based Fabry-Perot interferometer exhibited a concentration-specific reaction to a mixture of propane and nitrogen (37). ZIF-8 film fabrication involves no substrate modification, works at room temperature and facilitates control over the thickness with one growth cycle that takes less than an hour (37,38). In addition to being sensitive to organic vapours (36,37), ZIF-8 has been selected over other MOFs (and ZIFs) due to simplicity in fabrication and deposition of the thin film. The procedure for ZIF-8 film fabrication involves no substrate modification (37), works at room temperature and facilitates control over the thickness with one growth cycle that takes less than an hour. In addition, since ZIF-8 is hydrophobic no significant response to the relative humidity (even at relative humidity larger than 70%) is observed (39). We have recently demonstrated for the first time, to the best of our knowledge, proof of concept data for the detection VOCs using a LPG coated with ZIF-8 (39). A LPG based sensor coated with a ZIF-8 thin film exposed to methanol, ethanol and acetone vapours demonstrates a high sensitivity to all analytes tested, suggesting sensitivity towards low chain VOCs due to the small pore apertures (3.4 Å (35)).

However, before systems based on the technology can be widely deployed, it is essential that the sensor operates under optimised conditions in terms of both sensitivity and signal extraction. The research described here addresses these challenges. The sensitivity of the sensor is improved significantly by adjusting the grating period in such a way that the sensor operates precisely at the PMTP. This operation also facilitates the development of a novel signal processing method applied to the measured LPG spectrum. Higher sensitivity is obtained

when the sensor operates in the proximity of the PMTP associated with the occurrence of two attenuation bands in the spectrum, both of them associated with the same cladding mode. The relationship between the LPG spectrum and analyte concentration is usually tracked via the change in the central wavelength associated with distinct cladding modes. When two attenuation bands are present, the shift of the individual bands can be tracked or the difference between the central wavelengths related to those attenuation bands can be used for the evaluation of the sensor performance. The latter one gives the higher sensitivity (39). When the sensor is operating precisely at the PMTP a U-shaped band is present. In this case changes in the transmission at the central wavelength can be used for the measurement of target analytes (42). A novel alternative proposed here is that changes in the bandwidth of the U-shaped band can also be related to the target analyte. This approach is compared with alternatives based on monitoring the intensity and central wavelength changes.

The next section presents the method of manufacture of ZIF-8 films on LPGs with 2 different periods, one in the proximity of and one precisely at the PMTP; the test methodology for the sensors; and the novel signal processing method proposed. Section 3 shows results demonstrating the performance over a wide concentration range for different VOCs. Discussions and Conclusions follow in Sections 4 and 5 respectively.

## 2. Methodology

### 2.1 Materials

Zinc nitrate hexahydrate, 2-metyl-imidazole, methanol, ethanol, 2-propanol and acetone were purchased from Sigma-Aldrich. All of the chemicals were analytical grade reagents and used without further purification.

### 2.2 Long period grating fabrication

LPGs with grating periods of 109.0 and 109.5 μm and length of 30 mm (further referred to as Sensor A and Sensor B, respectively) were fabricated in photosensitive boron–germanium co-doped optical fibre (Fibercore PS750) using custom made amplitude masks made of 1Cr18Ni9Ti steel alloy. The grating periods of 109.0 and 109.5 μm were chosen so that the LPG operates in the proximity and exactly at the PMTP, respectively, after the deposition of the thin film of ZIF-8. The chemical sensitivity comparison performed for both sensors is further described in Section 2.4. Prior to exposure to the output from the laser, the polyacrylate

jacket of the fibre was mechanically removed over the section of the proposed grating. The laser used to side-illuminate optical fibre was a frequency quadrupled Nd:YAG laser emitting at a wavelength of 266 nm (Continuum minilite I), output power of 5 mW and beam diameter 3 mm. A cylindrical lens with a focal length of 100 mm was used to focus the beam into the core of the fibre, through an amplitude mask, producing a 3 mm long line focus aligned with the axis of the fibre (40). The use of an optical fibre with a short cut-off wavelength (~640 nm) ensures that resonance bands at their PMTP lie towards the red end of the visible spectrum, allowing the transmission spectrum of the LPG to be monitored using an inexpensive light source, halogen lamp, and a low-cost CCD spectrometer. The transmission spectrum of the optical fibre was recorded by coupling the output from a tungsten-halogen lamp (Ocean Optics HL-2000) into the fibre and analysing the transmitted light using a fibre coupled CCD spectrometer (Ocean Optics HR4000, with the resolution of 0.22 nm).

### 2.3 Sensor functionalization

The LPG was coated with ZIF-8 following the process described in (37,38) and demonstrated on the surface of an optical fibre LPG in our previous work (39). Briefly, the LPG was fixed in a custom designed holder to keep the LPG taut and straight. The LPG was placed inside a Petri dish and covered by the film forming solution (15 ml of 12.5 mM zinc nitrate hexahydrate and 15 ml of 25 mM 2-metyl-imidazole in methanol) for a period of 30 min. Then the LPG was washed by methanol and dried under nitrogen flow. The process was repeated to obtain thicker films consisting of 5 growth cycles. The transmission spectrum of the LPG was monitored during each deposition step. There was no indication that the film may be removed due to speed of the immersion as continuous building of the film was confirmed via the changes in the transmission spectrum.

### 2.4 Organic vapour testing

The response of the LPG to methanol, ethanol, 2-propanol and acetone was investigated with the fibre positioned in an environmental chamber composed of a closed polytetrafluoroethylene (PTFE) box (15x15x15 cm with a total volume of 3.375 L). The LPG was fixed 5 cm above the base. The chemical of interest (volume of 10 and 50 µl or 0.5 and 2 µl for experiments conducted with Sensor A and Sensor B, respectively) was injected from the top of the box by a pipette and the transmission spectrum was monitored and recorded. The concentration of the analyte was calculated according to the amount of the solution injected and the volume of the box. Sensor A was exposed to methanol, ethanol and acetone

concentrations ranging from 1,790 to 27900, 1240 to 24800 and 987 to 19700 ppm, respectively. Sensor B operates more closely to the PMTP and thus higher sensitivity was expected. This hypothesis was tested by exposing Sensor B to lower concentration of acetone and ethanol vapours in a range of 49 to 543 and 62 to 666 ppm, respectively. The temperature and relative humidity levels were simultaneously recorded using iButton® commercial data logger (iButton® Hygrochron Temperature/Humidity Logger DS1923, Maxim Integrated™). The temperature level was stable during the experiments with minor fluctuations up to 0.5 °C. All experiments have been conducted in a temperature and humidity controlled laboratory.

2.5 Signal processing

As described in Section 1, three methods for the evaluation of the changes in the LPG transmission spectrum are compared in this paper: via i) changes in the central wavelength difference, ii) changes in the transmission at the central wavelength of the U-shaped attenuation band and iii) changes in the bandwidth of the U-shaped attenuation band.

LODs have been calculated using the following equation

$$LOD = \frac{S_d}{m} \qquad \text{[EQ 2]}$$

where *LOD* indicates limit of detection, $S_d$ is the average standard deviation obtained over the values measured in stable conditions (at each concentration level) over the 2 min period and *m* is the slope of the calibration curve (a linear approximation was used for the range up to 10,000 ppm).

## 3. Results

3.1 Sensor fabrication

Figure 1a shows the transmission spectra of a bare LPG and a LPG coated with 5 layers of ZIF-8 for a grating period of 109.0 μm (Sensor A). The "U" shaped band of the $LP_{019}$ cladding mode splits into two attenuation bands after the deposition of the film. Figure 1b shows a grating period of 109.5 μm, where no attenuation band corresponding to the $LP_{019}$ cladding mode is observed before the coating process and which is developed only after the deposition of ZIF-8 (Sensor B). As discussed in section 2.2, this is precisely at the PMTP and is likely to

result in the highest sensitivity.

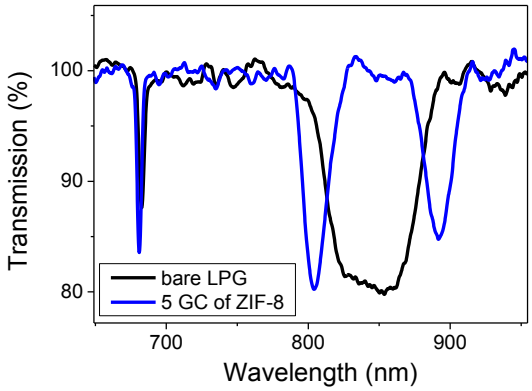


(a)

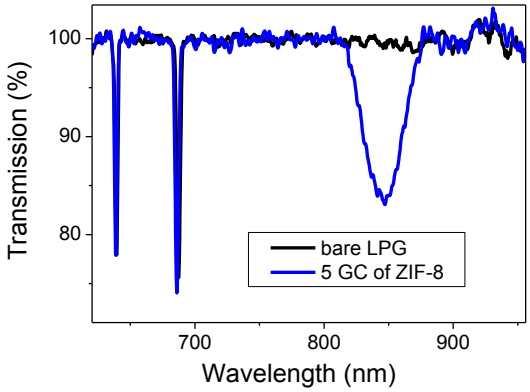


*(b)*

*Figure 1: Transmission spectrum of a LPG with period of a) 109.0 µm – Sensor A and b) 109.5 µm – Sensor B measured in air: uncoated (black) and coated with 5 growth cycles of ZIF-8 (blue), GC, growth cycle. Sensor A is close to the PMTP and Sensor B precisely at the PMTP.*

### 3.2 Sensor A: volatile organic compounds sensing

Sensor A was calibrated via three repeated measurements and its performance was evaluated via the change in central wavelengths difference method described in section 2.5. Without the presence of the U-shaped attenuation band, the other 2 signal processing methods described in section 2.5 cannot be applied (Figure 1a, blue line). The sensitivity to ethanol and acetone was observed to be higher than for methanol, Figure 2. At low concentrations and up to 5,000 ppm,

the sensor shows the highest sensitivity to ethanol, inducing a central wavelength shift of 12.34±1.97 nm at 4963 ppm.

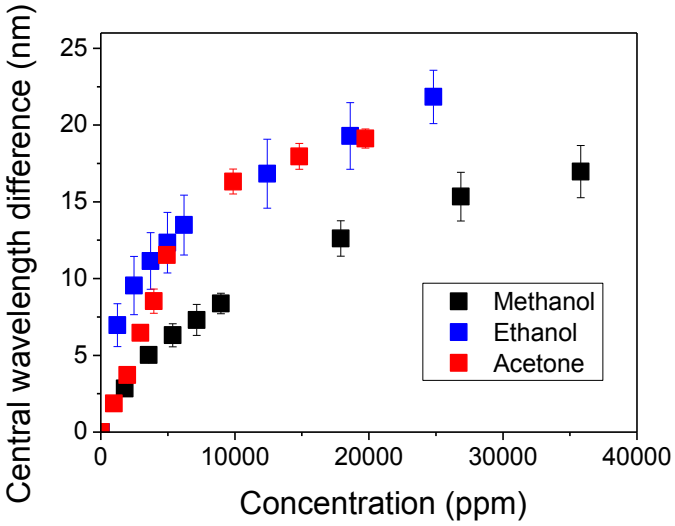


*(a)*

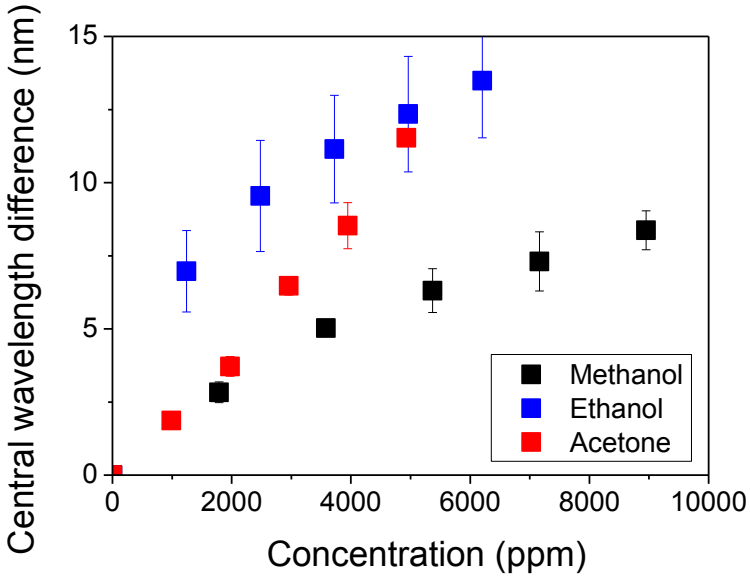


*(b)*

*Figure 2: Sensor A: calibration curves for methanol (black), ethanol (blue) and acetone (red). Error bars represent the standard deviation of the values taken over the three separate experiments b) shows the inset of a) where the data up to 10,000 ppm are shown for clarity.*

Higher sensitivity to all tested analytes was observed in comparison to the results presented in (39) measured using the central wavelengths difference corresponding to the LPG coated with 5 growth cycles of ZIF-8. For example, the change in the central wavelength difference induced by ~9,000 ppm of methanol vapour was measured to be 8.37 nm in comparison to 2.17 nm obtained in our preliminary work (39). The higher sensitivity of the current sensors is due to the smaller separation of the attenuation bands in air as the sensor operates closer to the PMTP.

The differences in the sensitivity can be associated with the size of the molecule, where the smaller methanol molecules have lower capture rate in the cavities at lower concentrations. The functional group can also play a role and can explain the bigger response of the sensor to ethanol in comparison to acetone at low levels up to 5,000 ppm. The shape of the curve indicates the saturation of the sensor at high concentrations over 20,000 ppm. For simplicity, a linear approximation is assumed in the range up to 10,000 ppm in order to calculate the LOD using Equation [2]. LODs of 164.4, 421.7 and 162.8 ppm were obtained for acetone, methanol and ethanol respectively using the data presented in Figure 2.

### 3.3 Sensor B: volatile organic compounds sensing

The high sensitivity of Sensor A to ethanol and acetone vapours leads to the further investigation of improving the LOD by operating the LPG precisely at the PMTP using a grating period of 109.5 μm. As described in section 2.4, as higher sensitivity was anticipated, lower concentrations of ethanol and acetone (62 to 666 and 49 to 543 ppm, respectively) were used. Due to the presence of the U-shaped band (Figure 2b, blue line) it is now possible to track changes in the spectrum due to a change in the transmission at the central wavelength and also the change in bandwidth of the attenuation band. Due to the absence of the dual attenuation bands, it is not possible to use the central wavelength difference method used in section 3.2.

The performance of Sensor B has been evaluated via the changes in transmission at the central wavelength. For instance, concentration of 543 ppm of acetone vapour induced a change of approximately 2 % in transmission at the central wavelength of Sensor B, Figure S1a. Similarly, a concentration of 666 ppm of ethanol caused approximately 3% change in transmission, Figure S1b. The response of Sensor B to acetone vapours in a range from 49 to 543 ppm based on the changes in the transmission at the central wavelength are shown in Figure 3a. Similarly, the response of Sensor B to ethanol vapours in range from 62 to 666 ppm is shown in Figure 2b. These values were used to calculate the standard the standard deviation of

the intensity changes 10 mV and for this reason the adequate change of 0.1 % in transmission has been used for the calculation of the LOD. LODs of 25.64 and 21.28 ppm have been calculated for acetone and ethanol respectively for Sensor B based on the change in transmission at the central wavelength of the attenuation band corresponding to $LP_{019}$ cladding mode.

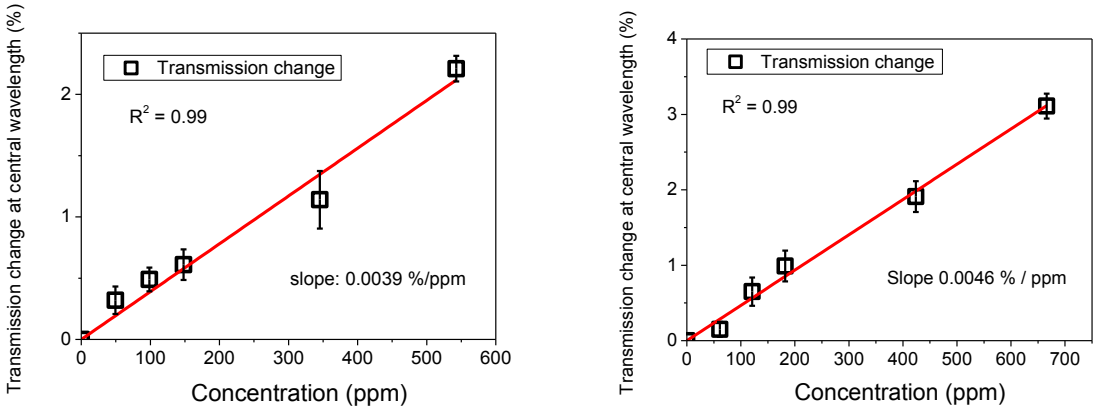


(a) (b)

*Figure 3: Sensor B: calibration curve based on the change in transmission loss (the error bars represented by the standard deviation of the value at the stable conditions at each concentration step are smaller than the data points) a) acetone and b) ethanol.*

As described in section 2.5, the change in the bandwidth of the U-shaped band represents a novel approach for the evaluation of LPG based sensors. Tracking the width of the attenuation band overcomes any intensity based issues as there is no need to track the absolute intensity at reference wavelength. The evolution of the differences in the width of the attenuation band corresponding to $LP_{019}$ cladding mode has been demonstrated in response to ethanol vapours in the range of 62 to 666 ppm, Figure 4a. The bandwidth was measured at the wavelengths corresponding to 85 % of transmission, as shown in detail for the left section of the attenuation band (in the region of 820 nm) in Figure 4b. As an example, the bandwidth increased from 54.68 to 66.27 nm in response to 666 ppm of ethanol, Figure 4.

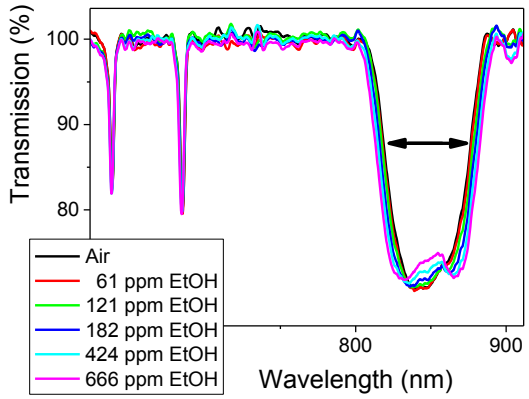


*(a)*

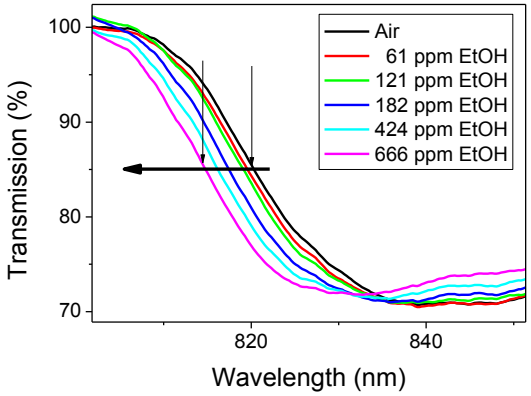


*(b)*

*Figure 4: Sensor B: a) Transmission spectra and b) left section of the attenuation band corresponding to $LP_{019}$ cladding mode in detail, measured in air (black), in response to 62 (red), 121 (green), 181 (blue), 424 (cyan) and 666 ppm of ethanol (magenta).*

The calibration curves (Figure 5) were calculated based on the change of bandwidth via the results of three repeated measurements. The slope of 0.018±0.0015 nm/ppm was obtained for ethanol, Figure 5. The error bar represents the standard deviation of the calculated slope value. Similarly, the response of Sensor B has been evaluated for acetone over the range of 49 to 543 ppm with a slope of width difference of 0.015±0.001 nm/ppm. The LOD of the sensor has been calculated in relation to a standard deviation of 0.1 nm and following Equation 2. LOD of 5.56 and 6.67 ppm was obtained for ethanol and acetone, respectively. The sensor's performance and dynamic change in time can also be tracked via the shift of the central wavelength of the $LP_{018}$ cladding mode. As an example, Sensor B responded even to the lowest concentration of 61 ppm of ethanol and showed a further shift of the central wavelength up to highest

concentration of 666 ppm of ethanol, inducing the shift of the central wavelength of 0.60 nm at 666 ppm, Figure S2.

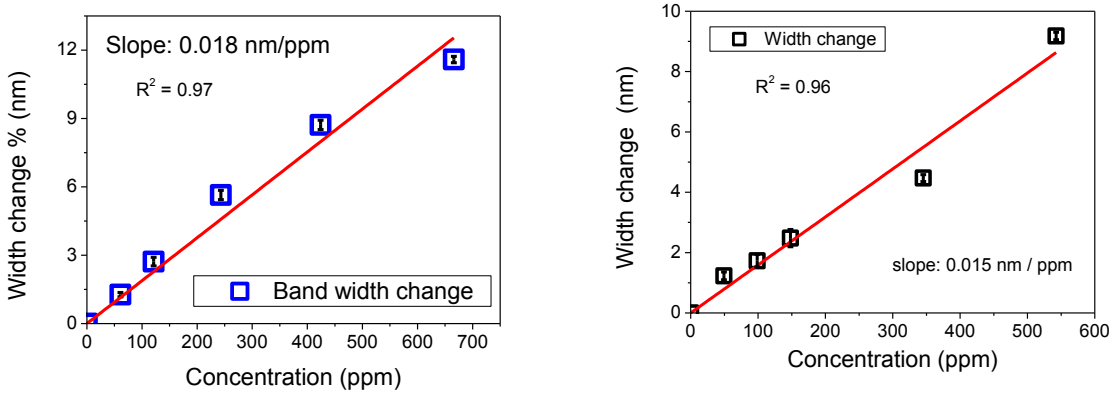


*(a)* *(b)*

*Figure 5: Sensor B: a) acetone and b) ethanol calibration curve based on the changes in band width (the error bars represented by the standard deviation of the value at the stable conditions at each concentration step are smaller than the data points).*

## 4 Discussion

The sensitivity of Sensor A and Sensor B using different data evaluation techniques over the range of analytes is compared in

. The obtained sensitivity for the ethanol vapour measurement fulfils the criteria for ethanol limit values for drivers in the range of 0.2-0.8 % in blood (the values differ across the countries. The conversion of those limits into the amount of ethanol in gas phase will give the range of 30-130 ppm (2).

The obtained sensitivity for the detection of acetone is sufficient to monitor occupational exposure in the workplace. The Health and Safety Executive in the UK states the exposure limits of 500 and 1500 ppm of acetone as a weighted average over 8 hours and 15 min respectively (43). Electrochemical based sensor represent the competing developing technology in a field of new acetone gas sensors, the LODs vary from 0.4 to 500 ppm, however, they suffer from high operating temperature (200-500 $^{o}$C) and sometimes were tested only in $N_2$ atmosphere (44). The concentration ranges from 1.7 ppm to 3.7 ppm could be detected in

breath of people with diagnosed diabetic conditions in comparison to 0.8 ppm measured in breath of healthy people (3). Furthermore, the LPG based sensors with current design can be used for measurement of acetone in breath for the monitoring of ketogenic diet and associated weight loss (range of 2-40 ppm) or diabetic ketoacidosis (75-1,250 ppm) (4).

The obtained LOD in a range of units of ppm for ethanol and acetone suggests the potential of the sensor for real world applications. Further improvement could be made by using a higher resolution spectrometer in combination with a new approach of data analysis (including the transmission, central wavelength and width change). The sub ppm level will be highly desired in health monitoring applications, e.g. breath analysis. The higher sensitivity could be also achieved using the thicker film and this hypothesis should be tested in future work. Although there is a clear cross sensitivity to different VOCs many of the tests can be designed to reduce this problem. It is expected however that one concentration will be significantly higher than the others for many applications. For example, in breath tests for alcohol consumption, ethanol levels will be two orders of magnitude higher in breath (when they reach the levels that break the law) in comparison to the other VOCs present in the breath. Similarly, patients suffering from ketoacidosis are expected to have much higher concentration of acetone in their breath in comparison to other VOCs. The implementation of the sensor into an array will enable in-situ measurement, e.g. for the occupational exposure, or any industrial monitoring, where a reference grating is necessary to subtract any temperature effect (45). The cross-sensitivity to water vapour in highly humid environment should also be included to test the possibility of using this sensor in breath analysis (46).

## 5. Conclusions

ZIF-8 films with controllable thickness have been deposited successfully onto the surface of an optical fibre LPG and the response of the transmission spectra has been characterized for different volatile organic compounds (ethanol, acetone and methanol). The importance of precisely setting the grating period so that the long period grating sensor operates exactly at the phase matching turning point has also been demonstrated. Furthermore three different signal processing methods for monitoring the change of the transmission spectra have been evaluated. The highest sensitivity has been obtained when the LPG operates precisely at the phase matching turning point and the bandwidth of the U-shaped attenuation band is measured. For example for ethanol this optimisation process results in the calculated limit of detection

reducing from 163 ppm to 5.6 ppm.

**Acknowledgment**:

This work was supported by the Engineering and Physical Sciences Research Council [grant numbers EP/N026985/1, EP/N025725/1].

## References

1. Wongrat E, Chanlek N, Chueaiarrom C, Samransuksamer B, Hongsith N, Choopun S. Low temperature ethanol response enhancement of ZnO nanostructures sensor decorated with gold nanoparticles exposed to UV illumination. Sensors Actuators, A Phys [Internet]. 2016;251:188–97. Available from: http://dx.doi.org/10.1016/j.sna.2016.10.022
2. Domènech-Gil G, Samà J, Pellegrino P, Barth S, Gràcia I, Cané C, et al. Gas nanosensors based on individual indium oxide nanostructures. Procedia Eng [Internet]. 2015;120:795–8. Available from: http://dx.doi.org/10.1016/j.snb.2016.07.084
3. Deng C, Zhang J, Yu X, Zhang W, Zhang X. Determination of acetone in human breath by gas chromatography-mass spectrometry and solid-phase microextraction with on-fiber derivatization. J Chromatogr B Anal Technol Biomed Life Sci. 2004;810(2):269–75.
4. Anderson JC. Measuring breath acetone for monitoring fat loss: Review. Obesity. 2015;23(12):2327–34.
5. Federal-Provincial Advisory Committe on Environmental and Occupational Health. Indoor Air Quality in Office Buildings : A Technical Guide. 1995. 1-57 p.
6. Parthibavarman M, Renganathan B, Sastikumar D. Development of high sensitivity ethanol gas sensor based on Co-doped SnO2 nanoparticles by microwave irradiation technique. Curr Appl Phys [Internet]. 2013;13(7):1537–44. Available from: http://dx.doi.org/10.1016/j.cap.2013.05.016
7. Ahmad MZ, Sadek AZ, Ou JZ, Yaacob MH, Latham K, Wlodarski W. Facile synthesis of nanostructured WO3 thin films and their characterization for ethanol sensing. Mater Chem Phys [Internet]. 2013;141(2–3):912–9. Available from: http://dx.doi.org/10.1016/j.matchemphys.2013.06.022
8. Ko H, Park S, An S, Lee C. Enhanced ethanol sensing properties of TiO2/ZnO core-shell nanorod sensors. Curr Appl Phys [Internet]. 2013;13:919–24. Available from: http://dx.doi.org/10.1016/j.cap.2013.01.020
9. Wang L, Fei T, Lou Z, Zhang T. Three-Dimensional Hierarchical Flowerlike α -Fe 2 O 3 Nanostructures : Synthesis and Ethanol-Sensing Properties. Appl Mater Interfaces. 2011;4689–94.
10. Wongrat E, Pimpang P, Choopun S. Comparative study of ethanol sensor based on gold nanoparticles: ZnO nanostructure and gold: ZnO nanostructure. Appl Surf Sci. 2009;256(4):968–71.
11. Shobin LR, Renganathan B, Sastikumar D, Park KC, Manivannan S. Pure and iso-butyl methyl ketone treated multi-walled carbon nanotubes for ethanol and methanol vapor sensing. IEEE Sens J. 2014;14(4):1238–43.
12. NaderiNasrabadi M, Mortazavi Y, Khodadadi AA. Highly sensitive and selective Gd2O3-doped SnO2 ethanol sensors synthesized by a high temperature and pressure

solvothermal method in a microreactor. Sensors Actuators, B Chem [Internet]. 2016;230:130–9. Available from: http://dx.doi.org/10.1016/j.snb.2016.02.045
13. Kersey AD. A Review of Recent Developments in Fiber Optic Sensor Technology. Opt Fiber Technol [Internet]. 1996;2:291–317. Available from: http://www.sciencedirect.com/science/article/pii/S106852009690036X
14. Cusano A, Consales M, Crescitelli A, Penza M, Aversa P, Veneri PD, et al. Charge transfer effects on the sensing properties of fiber optic chemical nano-sensors based on single-walled carbon nanotubes. Carbon N Y [Internet]. 2009;47(3):782–8. Available from: http://dx.doi.org/10.1016/j.carbon.2008.11.014
15. Elosúa C, Bariáin C, Matías IR, Arregui FJ, Luquin A, Vergara E, et al. Indicator immobilization on Fabry-Perot nanocavities towards development of fiber optic sensors. Sensors Actuators, B Chem. 2008;130(1):158–63.
16. Terrones SC, Aguado CE, Bariáin C, Carretero AS, Matías Maestro IR, Gutiérrez AF, et al. Volatile-organic-compound optic fiber sensor using a gold-silver vapochromic complex. Opt Eng. 2006;45(4):44401.
17. Zhang ZH, Lockwood R, Veinot JGC, Meldrum A. Detection of ethanol and water vapor with silicon quantum dots coupled to an optical fiber. Sensors Actuators, B Chem [Internet]. 2013;181:523–8. Available from: http://dx.doi.org/10.1016/j.snb.2013.01.070
18. Lokman MQ, Bin Abdul Rahim HR, Harun SW, Hornyak GL, Mohammed WS. Light backscattering (e.g. reflectance) by ZnO nanorods on tips of plastic optical fibres with application for humidity and alcohol vapour sensing. Micro Nano Lett [Internet]. 2016;11(12):832–6. Available from: http://digital-library.theiet.org/content/journals/10.1049/mnl.2016.0321
19. Manivannan S, Saranya AM, Renganathan B, Sastikumar D, Gobi G, Park KC. Single-walled carbon nanotubes wrapped poly-methyl methacrylate fiber optic sensor for ammonia, ethanol and methanol vapors at room temperature. Sensors Actuators, B Chem [Internet]. 2012;171–172:634–8. Available from: http://dx.doi.org/10.1016/j.snb.2012.05.045
20. Renganathan B, Sastikumar D, Srinivasan R, Ganesan AR. Nanocrystalline samarium oxide coated fiber optic gas sensor. Mater Sci Eng B Solid-State Mater Adv Technol [Internet]. 2014;186(1):122–7. Available from: http://dx.doi.org/10.1016/j.mseb.2014.03.018
21. Kavinkumar T, Sastikumar D, Manivannan S. Effect of functional groups on dielectric, optical gas sensing properties of graphene oxide and reduced graphene oxide at room temperature. RSC Adv [Internet]. 2015;5(14):10816–25. Available from: http://xlink.rsc.org/?DOI=C4RA12766H
22. Sharifpour-Boushehri S, Hosseini-Golgoo SM, Sheikhi MH. A low cost and reliable fiber optic ethanol sensor based on nano-sized SnO<inf>2</inf>. Opt Fiber Technol [Internet]. 2015;24:93–9. Available from: http://dx.doi.org/10.1016/j.yofte.2015.05.002
23. Ko Y, Tsai H, Lin K, Chen Y, Yang H. Reusable macroporous photonic crystal-based ethanol vapor detectors by doctor blade coating. J Colloid Interface Sci [Internet]. 2017;487:360–9. Available from: http://dx.doi.org/10.1016/j.jcis.2016.10.061
24. Konstantaki M, Klini A, Anglos D, Pissadakis S. An ethanol vapor detection probe based on a ZnO nanorod coated optical fiber long period grating. Opt Express. 2012;20(8):8472.
25. Kudo H, Sawai M, Suzuki Y, Wang X, Gessei T, Takahashi D, et al. Fiber-optic bio-sniffer (biochemical gas sensor) for high-selective monitoring of ethanol vapor using 335 nm UV-LED. Sensors Actuators, B Chem [Internet]. 2010;147(2):676–80. Available from: http://dx.doi.org/10.1016/j.snb.2010.03.066

26. Bearzotti A, Macagnano A, Papa P, Venditti I, Zampetti E. A study of a QCM sensor based on pentacene for the detection of BTX vapors in air. Sensors Actuators, B Chem [Internet]. 2017;240:1160–4. Available from: http://dx.doi.org/10.1016/j.snb.2016.09.097
27. Rego G. A review of refractometric sensors based on long period fibre gratings. Sci World J. 2013;2013.
28. James SW, Tatam RP. Optical fibre long-period grating sensors: characteristics and application. Meas Sci Technol. 2003;14(5):R49–61.
29. Topliss SM, James SW, Davis F, Higson SPJ, Tatam RP. Optical fibre long period grating based selective vapour sensing of volatile organic compounds. Sensors Actuators, B Chem. 2010;143(2):629–34.
30. Shu X, Zhang L, Bennion I. Sensitivity characteristics of long-period fiber gratings. J Light Technol. 2002;20(2):255–66.
31. Patrick HJ, Kersey AD, Bucholtz F. Analysis of the response of long period fiber gratings to external index of refraction. J Light Technol. 1998;16(9):1606–12.
32. Kumar P, Deep A, Kim K-H. Metal organic frameworks for sensing applications. TrAC Trends Anal Chem [Internet]. 2015;73:39–53. Available from: http://www.sciencedirect.com/science/article/pii/S0165993615001090
33. Kreno LE, Leong K, Farha OK, Allendorf M, Duyne RP Van, Hupp JT. Metal À Organic Framework Materials as Chemical Sensors. Chem Rev. 2012;112:1105–25.
34. Betard A and, Fischer RA. Metal À Organic Framework Thin Films : From Fundamentals to. 2012;1055–83.
35. Park KS, Ni Z, Côté AP, Choi JY, Huang R, Uribe-Romo FJ, et al. Exceptional chemical and thermal stability of zeolitic imidazolate frameworks. Proc Natl Acad Sci U S A. 2006;103(27):10186–91.
36. Demessence A, Boissière C, Grosso D, Horcajada P, Serre C, Férey G, et al. Adsorption properties in high optical quality nanoZIF-8 thin films with tunable thickness. J Mater Chem. 2010;20(36):7676.
37. Lu G, Hupp JT. Metal Organic Franeworks as Sensors A ZIF ( Based Fabry Perot Device as a Selective Sensor for Chemical Vapours and Gases.pdf. 2010;7832–3.
38. Lu G, Farha OK, Zhang W, Huo F, Hupp JT. Engineering ZIF-8 Thin Films for Hybrid MOF-Based Devices. Adv Mater. 2012;24:3970–4.
39. Hromadka J, Tokay B, James S, Tatam RP, Korposh S. Optical fibre long period grating gas sensor modified with metal organic framework thin films. Sensors Actuators, B Chem. 2015;221:891–9.
40. Hromadka J, Correia R, Korposh S. Fabrication of fiber optic long period gratings operating at the phase matching turning point using an amplitude mask. In: Proceedings of SPIE - The International Society for Optical Engineering. 2016.
41. Ye CC, James SW, Tatam RP. Simultaneous temperature and bend sensing with long-period fiber gratings. Opt Lett [Internet]. 2000;25(14):1007–9. Available from: http://www.ncbi.nlm.nih.gov/pubmed/18064255
42. Korposh S, Selyanchyn R, Yasukochi W, Lee SW, James SW, Tatam RP. Optical fibre long period grating with a nanoporous coating formed from silica nanoparticles for ammonia sensing in water. Mater Chem Phys [Internet]. 2012;133(2–3):784–92. Available from: http://dx.doi.org/10.1016/j.matchemphys.2012.01.094
43. Health and Safety Executive. EH4O / 2005 Workplace exposure limits EH4O / 2005 Workplace exposure limits. Eh40/2005. 2011;(March 2013):1–74.
44. Kao KW, Hsu MC, Chang YH, Gwo S, Andrew Yeh J. A Sub-ppm acetone gas sensor for diabetes detection using 10 nm thick ultrathin InN FETs. Sensors (Switzerland). 2012;12(6):7157–68.

45. Hromadka J, Korposh S, Partridge MC, James SW, Davis F, Crump D, et al. Multi-parameter measurements using optical fibre long period gratings for indoor air quality monitoring. Sensors Actuators, B Chem. 2017;244.
46. Hernandez FU, Morgan SP, Hayes-gill BR, Harvey D, Kinnear W, Norris A, et al. Characterization and Use of a Fiber Optic Sensor Based on PAH / SiO 2 Film for Humidity Sensing in Ventilator Care Equipment. 2016;63(9):1985–92.

***Table 1: Summary of ethanol gas fibre optic sensors (LOD – limit of detection)***

| **Sensor type** | **Sensor principle** | **Coating** | **Tested range** | **Sensitivity** | **Resp. time** | **LOD** | **Ref.** |
|---|---|---|---|---|---|---|---|
| Fabry–Perot interferometer (FPI) – film on the fibre tip | Δ of fibre-film reflectance | Single wall carbon nanotubes (SWCNT) | 63 and 73 ppm | 0.9 x$10^{-4}$ / ppm | ~ 3 min* | n/a | (14) |
| FPI - film on the fibre tip | Δ of fibre-film reflectance | SWCNT + cadmium arachidate | 63 and 73 ppm | 5x$10^{-4}$ / ppm | ~ 3 min* | n/a | (14) |
| FPI - film on the fibre tip | Δ in fluorescence; two sensors tested | vapochromic complex $[Au_2Ag_2(C_6F_5)_4(C_6H_5N)_2]$ | 1747 ppm (one value only) | 1 dB and 3 dB per 1747 ppm | 36 s / ~5 min | n/a | (15) |
| FPI - film on the fibre tip | Δ of fibre-film reflectance | vapochromic complex - 2,2'-bipyridine + Liquicoat® | 25-127 ppm | 0.0242 dB / ppm | 20 to 30 min | 2.74 ppm | (16) |
| Extrinsic sensor | Δ in fluorescence of nicotinamide adenine dinucleotide (NADH) | alcohol dehydrogenase (ADH) | 0.30 –300 ppm | 17.45 a.u. / ppm | n/a | n/a | (25) |
| Long period grating (LPG); period of 407 µm | Δ in intensity of the attenuation band | ZnO nanorods | ~ 50 Torr (saturated EtOH pressure) | ~ 4.4 dB | ~ 80 min | n/a | (24) |
| Cladding removed - poly-methyl methacrylate (PMMA) optical fibre | Δ in intensity at 678 nm | SWCNT | 12.5 -500 ppm | 0.26 a.u. / ppm | ~ 90 min | n/a | (19) |
| FPI - film on the fibre tip | Δ in luminescence from the QDs at 750 nm | fluorescent silicon quantum dots (Si- QDs) | 533 – 1,305 ppm in dry $O_2$ atmosphere | n/a | ~ 1 min | ~380 ppm | (17) |
| Cladding removed PMMA optical fibre | Δ in intensity at selected wavelengths | Multi-wall carbon nanotubes (MWCN) | 50-500 ppm | 0.52 a.u. / ppm (saturation at ~350 ppm) | n/a | n/a | (11) |
| Cladding removed PMMA optical fibre | Δ in intensity at selected wavelengths | $Sm_2O_3$ | 0 to 500 ppm | 76 x $10^{-3}$ au / ppm | 78 min | n/a | (20) |
| Cladding removed PMMA optical fibre | Δ in intensity at selected wavelengths | Graphene oxide | 100 to 500 ppm | 0.26 a.u. / ppm | n/a | n/a | (21) |
| Cladding removed silica optical fibre | Δ in power at selected wavelength | $SnO_2$ | 1000 to 20,000 ppm | ~0.02 µW / 1000 ppm (Saturated at 15,000 ppm) | 10-18 s | n/a | (22) |
| FPI - film on the fibre tip – PMMA fibre | Δ in intensity at selected wavelengths | ZnO nanorods | Saturated vapour | Δ 10.53 % in reflected intensity | n/a | n/a | (18) |
| Quartz crystal microbalance (QCM) | Δ frequency | organic polymer (pentacene) | 3074-15374 ppm | ~ 0.0064 Hz / ppm | ~30 s | n/a | (26) |

| | | | | | | | |
|---|---|---|---|---|---|---|---|
| Photonic crystal | Δ Bragg diffraction peak λ | Poly-acrylate type | EtOH/ water $p/p_0$ (0.2-1) | Max λ shift of 59 nm / pure EtOH gas | n/a | n/a | (23) |

***Table 2: Comparison of the performance of Sensor A and Sensor B towards organic vapours across the different evaluation techniques.***

| Sensor | Analyte | Conc. range [ppm] | Data evaluation technique | Sensitivity [nm/1000 ppm] | LOD [ppm] |
|---|---|---|---|---|---|
| Sensor A | MetOH | 1,790 to 27,900 | CW shift | 0.83 ± 0.08 | 421.7 |
| Sensor A | EtOH | 1,240 to 24,800 | CW shift | 2.58 ± 0.28 | 162.8 |
| Sensor A | Acetone | 987 to 19,700 | CW shift | 1.46 ± 0.06 | 164.4 |
| Sensor B | EtOH | 61 to 666 | Δ Bandwidth | 18 ± 1.5 | 5.56 |
| Sensor B | EtOH | 61 to 666 | Δ Transmission | 4.5 ± 0.2** | 21.28 |
| Sensor B | Acetone | 49 to 543 | Δ Bandwidth | 15 ± 1 | 6.67 |
| Sensor B | Acetone | 49 to 543 | Δ Transmission | 3.9 ± 0.2** | 25.64 |

* The linear response approximation was assumed for the sensitivity calculation.
** The units are transmission percent loss per 1000 ppm.